ELSEVIER

Thermochimica Acta 269/270 (1995) 491–506

thermochimica acta

Thermoanalytical study of synthesis of mixed lithium cobalt oxides ☆

M. Carewska, A.Di Bartolomeo [a], S. Scaccia *

Dipartimento Energia-Settore Tecnologie Energetiche Avanzate [a] Dipartimento Innovazione-Settore Nuovi Materiali, ENEA C.R.E. Casaccia, Via Anguillarese 301, I-00060 Rome, Italy

Received 8 November 1994; accepted 8 May 1995

Abstract

The synthesis of $LiCoO_2$ from different precursor mixtures, such as Li_2CO_3–Co_3O_4, $Li(CH_3COO)\cdot 2H_2O$-Co_3O_4, Li_2CO_3-$2CoCO_3\cdot 3Co(OH)_2$ and $Li(CH_3COO)\cdot 2H_2O$-$Co(CH_3COO)_2\cdot 4H_2O$ in air has been studied by means of TG, DTG and DTA techniques. The thermal events have been characterized by X-ray diffraction and chemical analysis. It is suggested that the synthesis proceeds through reaction between lithium carbonate and cobalt oxide intermediates. A lower synthesis temperature has been observed in the case of acetate precursors. The effect of the precursor on the electrical properties of the samples has been also studied. Measurements of electrical conductivity in the temperature range 600 to 900°C in air show typical semiconductive behaviour for all the samples of $LiCoO_2$. The Arrhenius plots show two linear regions with a temperature break due to phase transition near 850°C. The two values of activation energies in the temperature ranges 600–820 and 850–900°C have been found to be similar for all the samples, suggesting that the conduction behaviour should not be influenced by the nature of the precursor.

Keywords: Electrical conductivity; $LiCoO_2$; Synthesis; Thermal analysis

1. Introduction

Over the past ten years mixed lithium cobalt oxides gained interest for possible application as cathode electrodes in technologies such as secondary lithium batteries

* Corresponding author.

☆ Presented at the 6th European Symposium on Thermal Analysis and Calorimetry, Grado, Italy, 11–16 September 1994.

SSDI 0040-6031(95)02532-4

and more recently, molten carbonate fuel cells (MCFCs) [1, 2]. The studies on the electrochemical properties of this material have outlined that there exists a close relationship between the behaviour as cathode electrode and the electrical properties, namely modification in the electronic structure provided by the deintercalation process of lithium ions in the lattice causes a change of the behaviour of conduction from semiconductor to metallic [3, 4].

Furthermore, the electrochemical behaviour has been reported to depend on the preparation methods used for synthesis of the material. The first studies relating to preparation routes of $LiCoO_2$ for batteries were conducted by Mizushima et al. [5], who synthesized $LiCoO_2$ by solid state reaction of lithium carbonate with cobalt carbonate. By then, novel synthetic routes had been investigated, including spray-drying, sol–gel process and reaction in molten salts [6–9]. Yoshio et al. [8] found that $LiCoO_2$ from cobalt–organic acid complexes showed better electrochemical properties than that prepared by the conventional method.

In the framework of a project aimed at developing new cathode materials for MCFC, the present paper reports investigations on the effect of different precursors on the synthesis and electrical properties of $LiCoO_2$.

2. Experimental

2.1. Materials and apparatus

The precursors were all analytical reagent grade and analysed for cobalt and lithium content by atomic absorption spectroscopy (Varian SPECTRAA 10). Homogeneous equimolar mixtures: $Li(CH_3COO)\cdot 2H_2O$ (BDH GPR)–Co_3O_4 (Aldrich p.a), Li_2CO_3 Carlo Erba RPE)–Co_3O_4, Li_2CO_3–$2CoCO_3\cdot 3Co(OH)_2\cdot xH_2O$ (basic cobalt carbonate) (Carlo Erba RPE) and $Li(CH_3COO)\cdot 2H_2O$–$Co(CH_3COO)_2\cdot 4H_2O$ (Fluka p.a) were obtained by grinding the precursors with acetone in a planetary mill for 2 h.

Thermal analysis measurements were carried out on the single precursors and their mixtures using a DuPont 2000 Thermal Analysis System with 1600 DTA and 951 TGA modules. Thermogravimetry (TG) on about 20 mg of sample was carried out in dynamic air at flow rate of 50 ml min^{-1} and at heating rates of 5 or 10°C min^{-1}. A sample weight of 30 ± 5 mg was used for DTA analysis, which was carried out in static air and dynamic N_2 and O_2 at flow rate of 50 ml min^{-1} and at heating rate of 10°C min^{-1}, unless specified differently. α-Alumina powder was used as standard reference material.

The mixtures were also heated in a separate furnace using the same temperature programme. The end products and the intermediates obtained at different temperatures were characterized by X-ray diffraction analysis using an Ital-Structures 1S-86 diffractometer with a CoKα radiation source. The diffraction patterns were matched with ASTM cards [10].

The obtained powders were washed in cold water until free from soluble lithium and cobalt compounds. Then the residue was dried, dissolved in HCl and analysed by atomic absorption spectrometry for the determination of the Li/Co molar ratio.

The precursor mixtures were calcined at 650°C for 10 h, pelletized under a pressure of 100 mPa and sintered in air at 900°C for 10 h. The densities were about 90% of theoretical ones. XRD data revealed that the obtained pellets were single phase.

Electrical conductivity measurements were conducted on sintered pellets by a four gold points probe d.c. van der Pauw method [11] in the temperature range 600 to 900°C in different atmospheres (O_2, air and N_2).

3. Results

3.1. *Synthesis of* $LiCoO_2$ *from different precursors*

In Table 1 are summarized the experimental and calculated weight losses corresponding to the postulated reaction sequences between the reactants. The thermal events have been identified by comparison with the thermograms of the single precursors and by characterization of the intermediates obtained at different temperatures using X-ray diffraction (Fig. 1a–d) and chemical analysis (Table 1).

Li_2Co_3–Co_3O_4

The TG–DTG curves of a mixture of Li_2CO_3 and Co_3O_4 recorded at 5°C min^{-1} in air are shown in Fig. 2a. The DTG curve reveals a broad peak at 550°C, with a shoulder on the high-temperature side, which can be ascribed to formation of $LiCoO_2$. XRD patterns of the mixture heated at 400°C show weak reflections of the $LiCoO_2$ phase in addition to the most intense lines of Co_3O_4 and lithium carbonate, whereas the mixture heated at 700°C shows $LiCoO_2$ as the major component with minor presence of the starting reactants. In Fig. 2b are shown the DTA curves obtained at different heating rates. The curves show a small exothermic peak between 200 and 270°C, which is absent in the thermogram of the single precursors. An exothermic peak with an onset temperature of 650°C is recognized on the DTA curve at 20°C min^{-1}. The endothermic peak with maximum at 723°C is due to the melting of lithium carbonate and increases with increasing heating rate.

$Li(CH_3COO)\cdot 2H_2O$–Co_3O_4

The TG curve of the mixture of $Li(CH_3COO)\cdot 2H_2O$ and Co_3O_4 shows five steps of weight loss, with peaks in the derivative curve located at 62, 83, 140, 349 and 474°C (Fig. 3a). The steps between ambient temperature and 200°C are due to dehydration of lithium acetate dihydrate. This process is accompanied by endothermic overlapping peaks with maxima at 67, 99, 136 and 147°C on the DTA curve (Fig. 3b). The step between 220 and 380°C, followed by a slight weight increase, is accompanied by a strong exotherm at 361°C with a shoulder on the high-temperature side. XRD patterns of the mixture heated at 345°C show weak reflections of the $LiCoO_2$ phase along with the most intense lines of Co_3O_4. This results in a higher experimental weight loss compared to that corresponding to the postulated decomposition of lithium acetate (see Table 1). These findings may be explained by considering that the lithium acetate melts just before decomposition into lithium carbonate (endotherm peak with

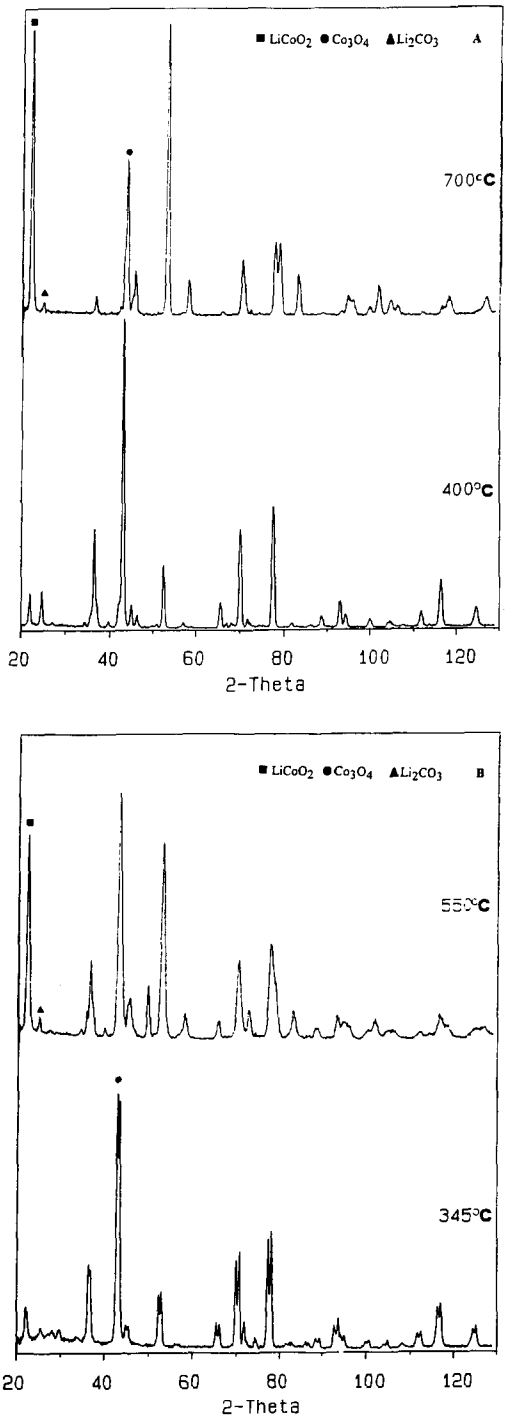

Fig. 1. X-ray patterns of precursor mixtures heated at different temperatures: Li_2CO_3–Co_3O_4 mixture (a); $Li(CH_3COO)\cdot 2H_2O$–Co_3O_4 mixture (b); Li_2CO_3–basic cobalt carbonate mixture (c); $Li(CH_3COO)\cdot 2H_2O$–$Co(CH_3COO)_2\cdot 4H_2O$ mixture (d).

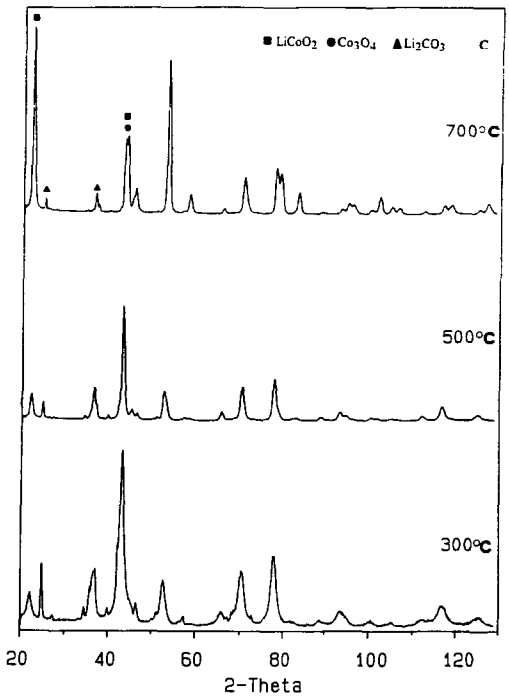

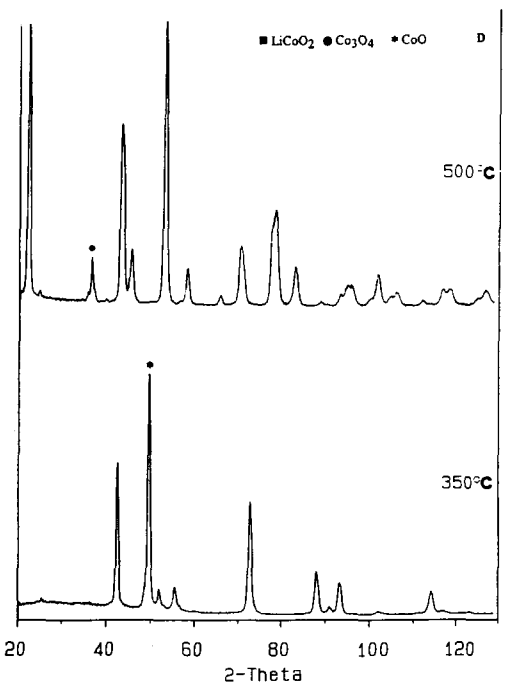

Fig. 1. (*Continued*).

Table 1
Decomposition scheme from TGA data of the mixtures and chemical analysis results

Decomposition reaction	Temperature range/°C	No of steps	Weight loss/%		Temperature /°C	Chemical analysis/wt%			
			Calc.	Exper.		water		residue	
						Li	Co	Li	Co
Li_2CO_3–Co_3O_4					400	5.4	<D.L[a]	0.1	50.0
					700	0.06	<D.L[a]	7.03	60.7
i) $3Li_2CO_3+2Co_3O_4 \rightarrow 6LiCoO_2+2CO_2+CO$	400–700	I	16.57	16.50					
$Li(CH_3COO)\cdot 2H_2O$–Co_3O_4									
$3Li(CH_3COO)\cdot 2H_2O+Co_3O_4 \rightarrow 3LiCoO_2+\ldots$	30–950		46.31	45.80	345	5.4	<D.L[a]	0.2	45.0
i) $3Li(CH_3COO)\cdot 2H_2O \rightarrow 3Li(CH_3COO)+2H_2O$	30–200	I, II, III	19.75	16.23	550	1.9	<D.L[a]	4.5	57.7
				3.00					
ii) $3Li(CH_3COO) \rightarrow 3/2Li_2CO_3+\ldots$	220 380	IV	15.95	17.54					
iii) $3/2Li_2CO_3+Co_3O_4 \rightarrow 3LiCoO_2+CO_2+1/2CO$	380–550	V	10.61	9.00					
Li_2CO_3–$2CoCO_3\cdot 3Co(OH)_2\cdot xH_2O$									
$5/2Li_2CO_3+2CoCO_3\cdot 3Co(OH)_2xH_2O \rightarrow 5LiCoO_2+\ldots$	30–900		30.23	30.72	300	5.4	0.06	0.1	45.0
i) $2CoCO_3\cdot 3Co(OH)_2\cdot xH_2O \rightarrow 5/3Co_3O_4+\ldots$	30–300	I	16.44	16.52	500	4.0	<D.L[a]	1.0	63.7
ii) $5/2Li_2CO_3+5/3Co_3O_4 \rightarrow 5LiCoO_2+2CO_2+1/2CO$	300–500	II	13.78	6.60	700	1.0	<D.L[a]	5.3	60.7
	500–700	III		7.60					
$Li(CH_3COO)\cdot 2H_2O$–$Co(CH_3COO)_2\cdot 4H_2O$									
$Li(CH_3COO)\cdot 2H_2O+Co(CH_3COO)_2\cdot 4H_2O \rightarrow LiCoO_2+\ldots$	30–950		72.12	71.40	350	5.4	0.07	0.1	55.0
i) $Co(CH_3COO)_2\cdot 4H_2O \rightarrow Co(CH_3COO)_2+4H_2O$	30–200	I, II, III	30.76	30.09	500	1.0	<D.L[a]	5.3	60.7
ii) $Li(CH_3COO)\cdot 2H_2O \rightarrow Li(CH_3COO)+2H_2O$	200–350	IV, V, VI	27.57	35.77					
iii) $Co(CH_3COO)_2 \rightarrow 1/3Co_3O_4+\ldots$			8.28						
iv) $Li(CH_3COO) \rightarrow 1/2Li_2CO_3\ldots.$	350–500	VII	5.51	5.50					
v) $1/2Li_2CO_3+1/3Co_3O_4 \rightarrow LiCoO_2+1/2CO_2+1/2CO$									

[a] D.L = detection limit $< 2 \times 10^{-4}$ wt%

onset temperature of 287 °C) promoting the beginning of the reaction with cobalt oxide. The step between 380 and 550°C, accompanied by a small exothermic peak with a maximum at 457°C, might be related to reaction of the freshly-formed lithium carbonate with Co_3O_4 to form $LiCoO_2$. XRD patterns of the mixture heated at 550°C show an increase in the intensity of the characteristic lines of $LiCoO_2$ along with lines of lithium carbonate and cobalt oxide. The final event on the DTA curve occurs at 850°C; this can be ascribed to a phase transition, as will be discussed later.

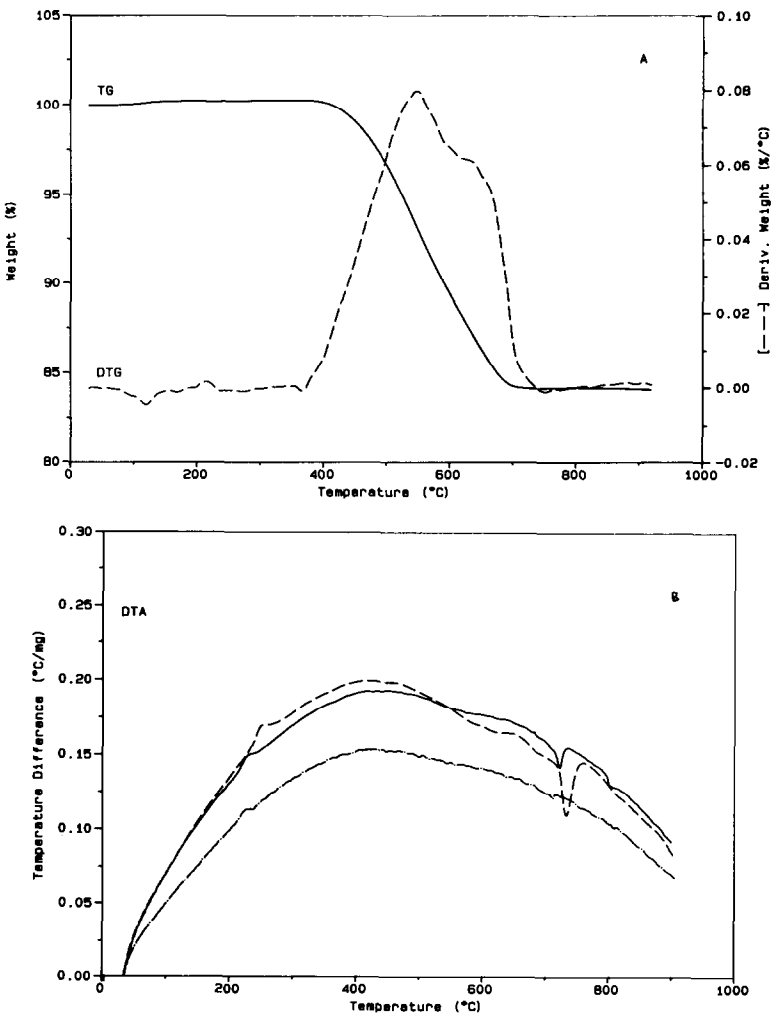

Fig. 2. TG–DTG curves of Li_2CO_3–Co_3O_4 mixture at 5 °C min^1 in air (a); DTA curves of Li_2CO_3–Co_3O_4 mixture at (–·–) 5, (—) 10 and (– –) 20 °C min^{-1} in air (b).

Li_2CO_3–*basic cobalt carbonate*

The TG–DTG curves of the mixture of lithium carbonate and basic cobalt carbonate are shown in Fig. 4a. There are three steps of weight loss with peaks in the derivative curve located at 267, 466 and 690 °C. The first step, between ambient temperature and 300 °C, is due to the decomposition of basic cobalt carbonate into Co_3O_4. This process is characterized by an endothermic peak with maximum at 279 °C in the DTA trace (Fig. 4b). XRD patterns of the mixture heated at 300 °C show weak reflections of $LiCoO_2$ in addition to the most intense lines of Co_3O_4 and lithium carbonate. The two

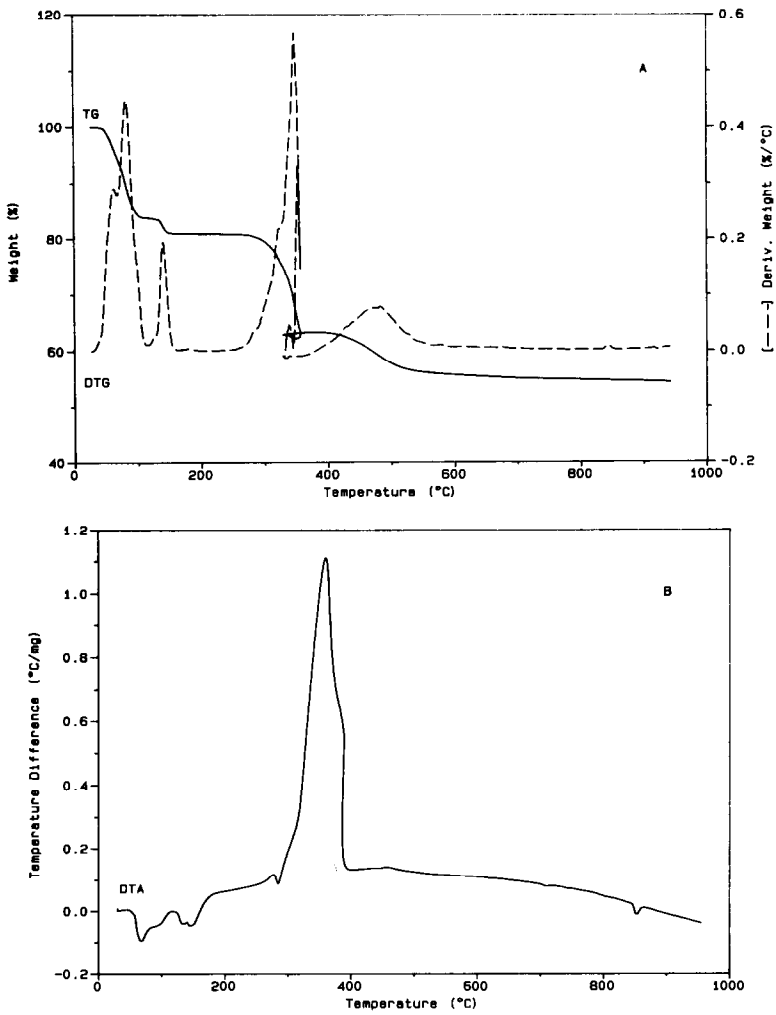

Fig. 3. TG–DTG curves (a) and DTA curve (b) of $Li(CH_3COO)\cdot 2H_2O$–Co_3O_4 mixture at 10 °C min^{-1} in air.

consecutive steps from 300 to 700°C are due to the reaction of freshly-formed cobalt oxide with lithium carbonate to form $LiCoO_2$ and subsequent decomposition of unreacted lithium carbonate, respectively. XRD patterns of the mixtures heated at 500 and 700°C, show a decrease of intensity of lines of reactants and an increase of the characteristic lines of the $LiCoO_2$ phase.

$Li(CH_3COO)\cdot 2H_2O$–$Co(CH_3COO)_2\cdot 4H_2O$

The TG–DTG curves of the mixture of lithium and cobalt acetates are shown in Fig. 5a. There are seven steps of weight loss with peaks in the derivative curve located at 62, 85, 115, 264, 288, 305 and 415°C. The steps from ambient temperature to 200°C are due to dehydration of dihydrated lithium and tetrahydrated cobalt acetates. These processes are accompanied by overlapping endothermic effects at 61, 95 and 146°C on the DTA curve (Fig. 5b). The steps from 200 to 350°C are ascribed to the decomposition of acetate into cobalt oxide and lithium carbonate. These weight losses have been associated with exothermic effects at 260 and 380°C. XRD patterns of the mixture heated at 350°C display only the characteristic lines of CoO, because it is not easy to detect the poorly crystalline freshly-formed lithium carbonate. The step between 350 and 500°C might be related to the reaction of lithium carbonate and cobalt oxide intermediates to form $LiCoO_2$. XRD patterns of the mixture heated at 500°C confirm that $LiCoO_2$ become the predominant phase. The endothermic peak at 845°C is recognized.

3.2. *Thermal stability of* $LiCoO_2$ *materials*

The thermal stability of samples of $LiCoO_2$ has been investigated in air by DTA analysis. An endotherm effect in the range 840–860°C appears in all the samples (Fig. 6a). This process is reversible as indicated by the exothermic peak on the DTA curves of cooling, which is shifted to lower temperature, at about 800°C (Fig. 6b). On heating and cooling repeatedly the positions of the endothermic and exothermic peaks remain unchanged. It is worth noting that the endothermic peak is similar to those observed in the thermograms of the precursor mixtures. In Fig. 7 are shown the DTA curves of $LiCoO_2$ formed from carbonate precursors in different atmospheres. It can be seen that the position of the endotherm peak is shifted to higher temperatures in the oxygen atmosphere and to lower temperatures in the nitrogen atmosphere.

3.3. *Electrical conductivity*

The variation of electrical conductivity with temperature has been studied in the temperature range 600–900°C. The data followed the exponential equation $\sigma = \sigma_0/T \exp(-E_a/kT)$ typical of semiconducting behaviour, where σ_0 is a pre-exponential factor, E_a the activation energy for conduction and k the Boltzman constant. The Arrhenius plots are given in Fig. 8. A break in the $\ln\sigma T - 1/T$ curves occurs around 850°C. The activation energies E_a along with pre-exponential factors calculated from the slope and intercept of the two linear portions of Fig. 8, respectively, are given in

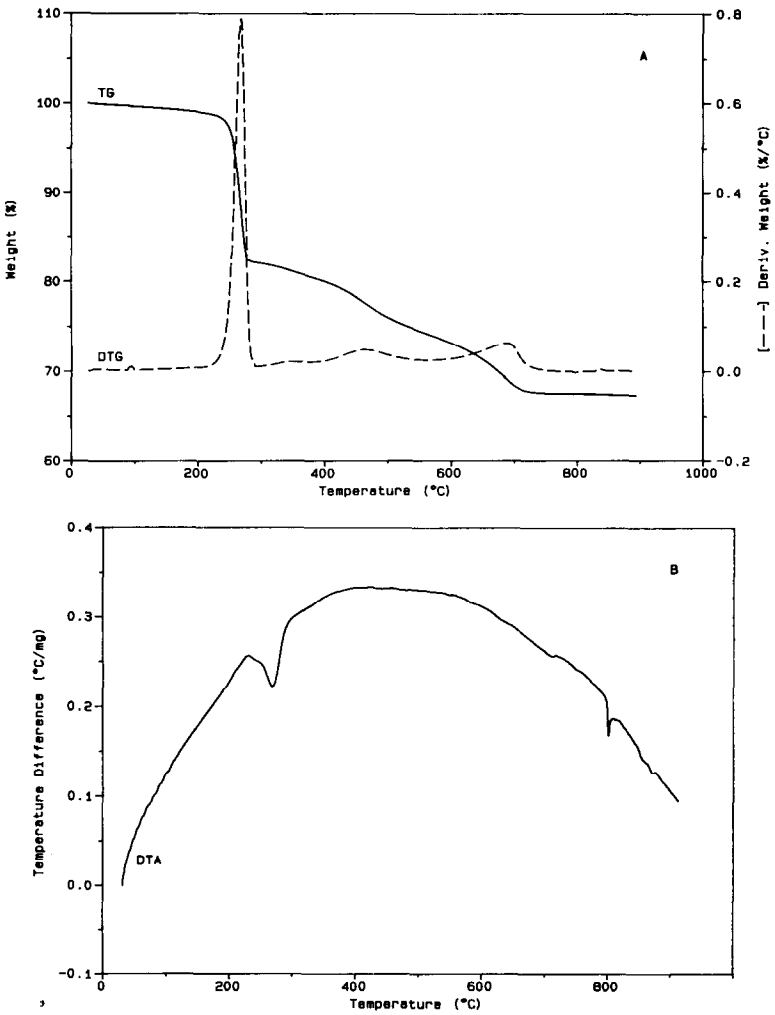

Fig. 4. TG–DTG curves (a) and DTA curve (b) of Li_2CO_3–basic cobalt carbonate mixture at 10 °C min^{-1} in air.

Table 2. The activation energies in the temperature regions 600–820 and 850–900 °C have been found to be significantly different. In the low-temperature region the value of the activation energy ($E_a = 0.37$ eV) is typical of extrinsic conduction. In the high temperature region the activation energy has been calculated to be 1.15 eV and the electrical conductivity becomes nearly independent of oxygen partial pressure (Fig. 9). The temperature-dependence of resistivity of samples of $LiCoO_2$ in air is given in Fig. 10. The curves show a sharp drop in resistivity near 850 °C and an hysteresis can be noticed during the heating and cooling cycles.

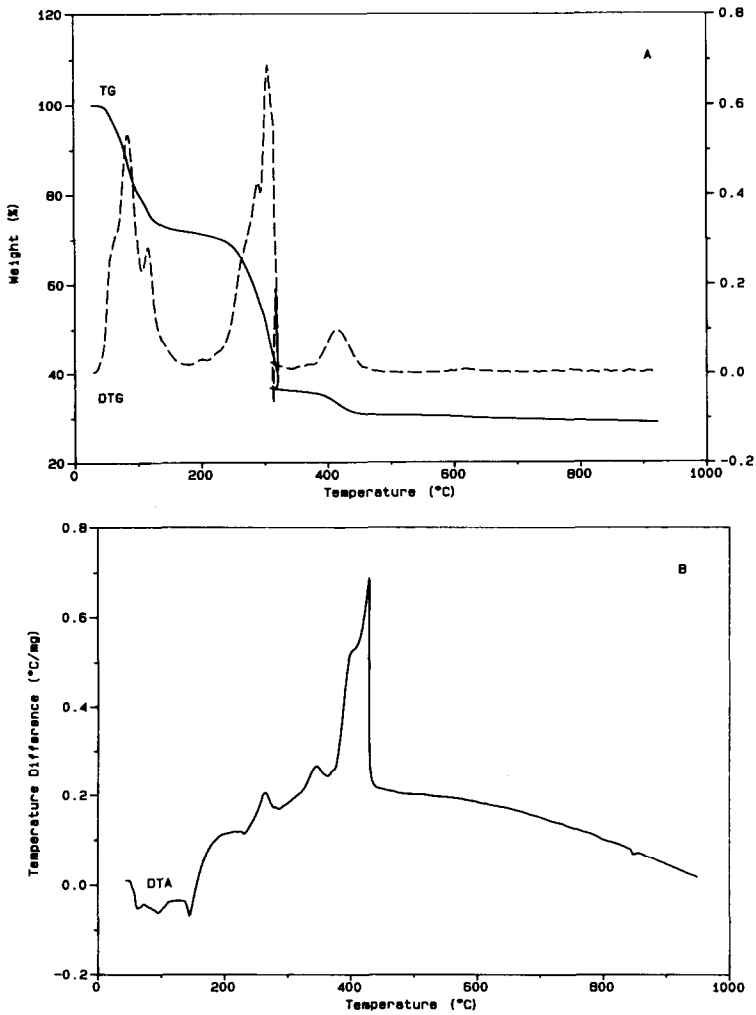

Fig. 5. TG–DTG curves (a) and DTA curve (b) of $Li(CH_3COO)\cdot 2H_2O$–$Co(CH_3COO)_2\cdot 4H_2O$ mixture at 10°C min^{-1} in air.

4. Discussion

Our experimental results on the formation of $LiCoO_2$ from different precursors indicate that the synthesis takes place through the reaction of lithium carbonate and cobalt oxide. However, the solid state reaction of lithium carbonate and cobalt oxide begins at 400°C and is not completed until the temperature of 700°C is reached, indicating poor reactivity. In the case of the mixture of carbonates the $LiCoO_2$ phase is already detected at 300°C indicating that the cobalt oxide, formed in situ during

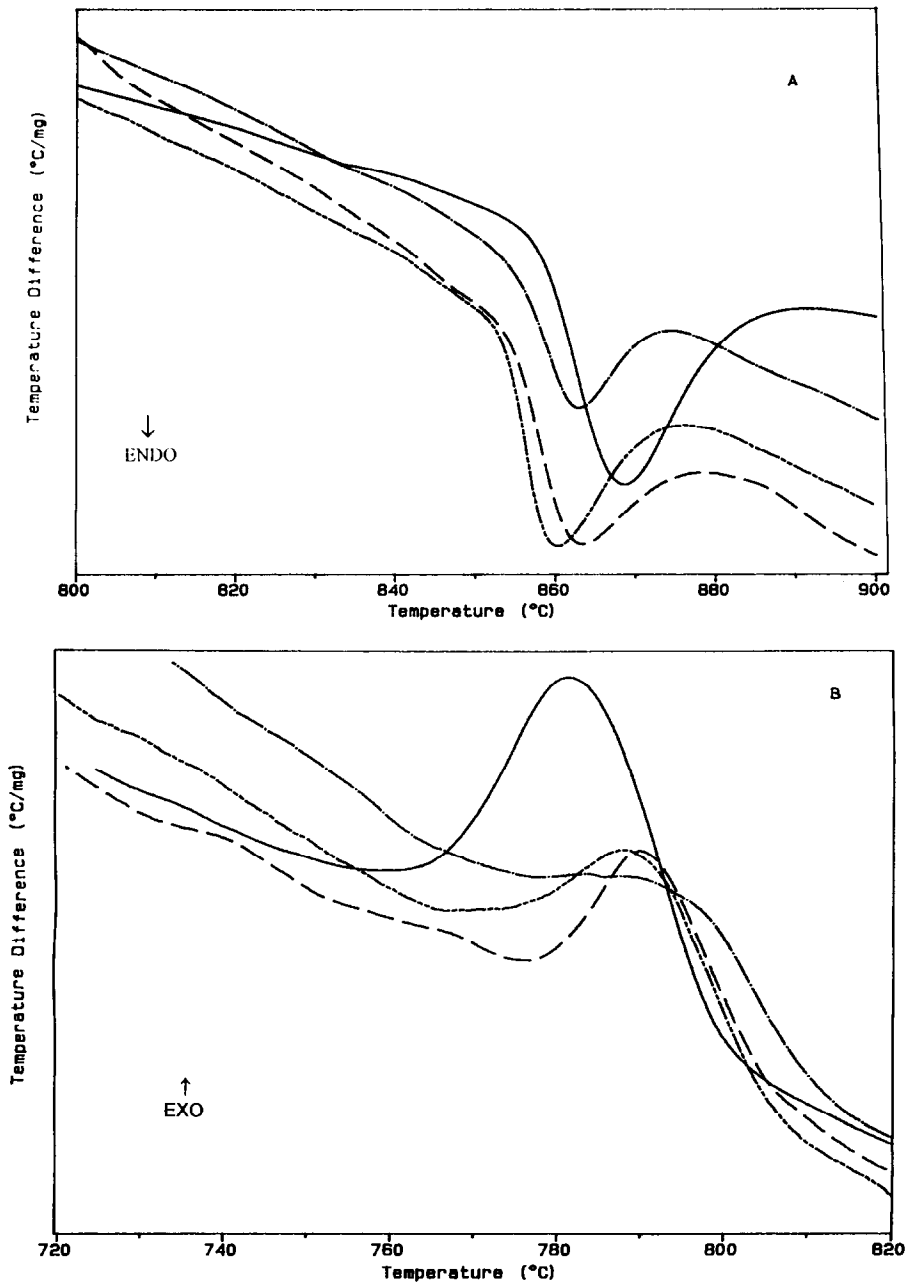

Fig. 6. DTA curves of samples of $LiCoO_2$ in air at heating rate (a) and cooling rate (b) of 10°C min^{-1}: Li_2CO_3–Co_3O_4 precursors (–·–); $Li(CH_3COO)\cdot 2H_2O$–Co_3O_4 precursors (– –); Li_2CO_3–basic cobalt carbonate precursors (— — — —); $Li(CH_3COO)\cdot 2H_2O$–$Co(CH_3COO)_2\cdot 4H_2O$ precursors (—).

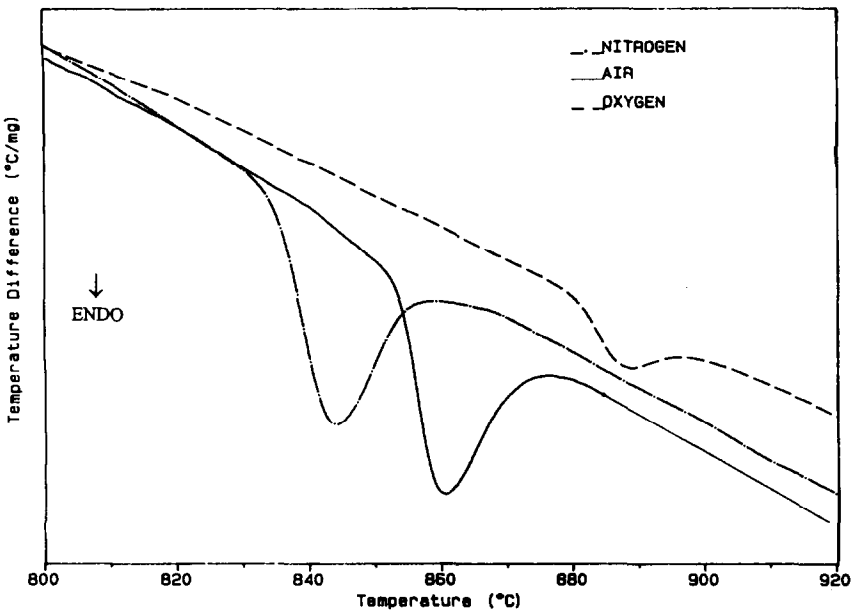

Fig. 7. DTA curves of $LiCoO_2$ from carbonate precursors under different atmospheres at heating rate of 10°C min^{-1}.

thermal decomposition of carbonate, is more reactive than the cobalt oxide used as precursor. It is worth noting that completion of the reaction of formation of $LiCoO_2$ is reached at a lower temperature when the acetate precursors are used. This probably occurs because the acetates melt and decompose at lower temperatures than the other precursors, producing intermediate species that rapidly react to give $LiCoO_2$. As seen previously, the samples exhibit extrinsic behaviour in the low temperature region, followed by a sharp increase in conductivity near 850°C, which may reflect the existence of a phase transition. The transition temperatures observed in the DTA heating and cooling curves are in fair agreement with those observed from electrical resistivity measurements. To the best of the author's knowledge, this transition has not been reported before. Usually, when $LiCoO_2$ is synthesized at temperatures as high as 900°C it has a ordered layered rocksalt structure in which lithium and cobalt cations reside in alternate layers in octahedral sites between the cubic-close-packed oxygen planes [12]. However, recent studies on stoichiometric $LiCoO_2$ have shown that an LT-$LiCoO_2$ synthesized at low temperature (400°C) adopts a slightly modified structure intermediate between an ideal layered and an ideal lithiated spinel structure [13–15]. Unfortunately, the two structures are hardly distinguishable using X-ray diffraction powder patterns [4]. Hence, it is here assumed that the phase transition near 850°C is a spinel–rocksalt type similar to that reported for the systems Co_3O_4–CoO [16] and $Li_{0.35}Co_{2.65}O_4$ [17].

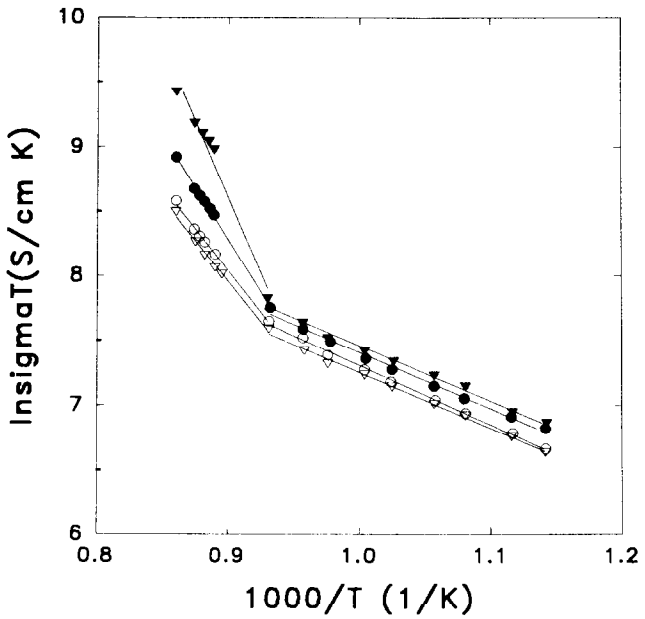

Fig. 8. LnσT versus reciprocal of absolute temperature of samples of $LiCoO_2$ formed from Li_2CO_3–Co_3O_4 precursors (○); $Li(CH_3COO)\cdot 2H_2O$–Co_3O_4 precursors (Δ); Li_2CO_3–basic cobalt carbonate precursors (●); $Li(CH_3COO)\cdot 2H_2O$–$Co(CH_3COO)_2\cdot 4H_2O$ precursors (▲).

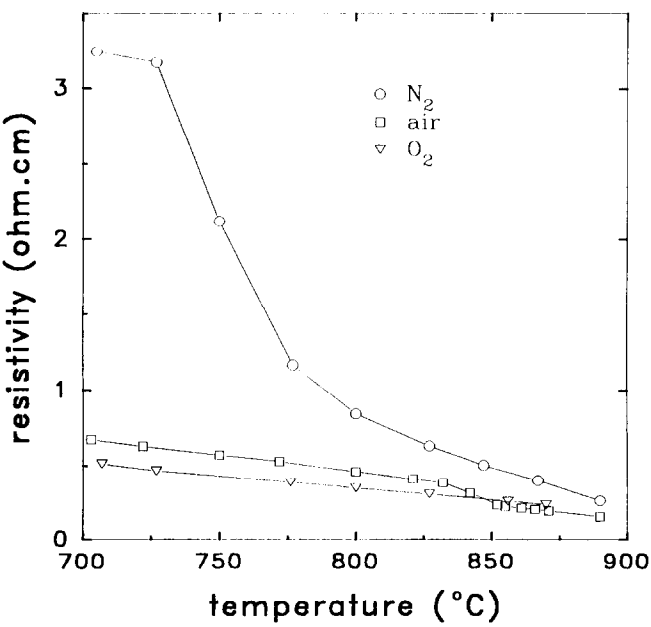

Fig. 9. Temperature-dependence of resistivity in different atmospheres for $LiCoO_2$ formed from carbonate precursors.

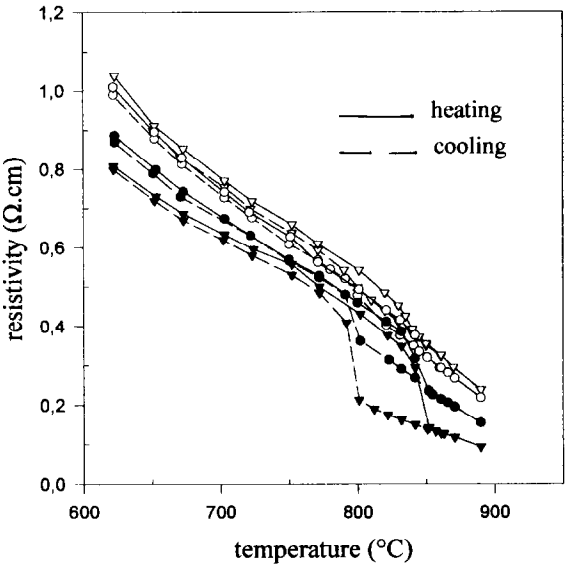

Fig. 10. Temperature-dependence of resistivity in air of samples of $LiCoO_2$ formed from Li_2CO_3–Co_3O_4 precursors (○); $Li(CH_3COO)\cdot 2H_2O$–Co_3O_4 precursors (Δ); Li_2CO_3–basic cobalt carbonate precursors (●); $Li(CH_3COO)\cdot 2H_2O$–$Co(CH_3COO)_2\cdot 4H_2O$ precursors (▲).

Table 2
Activation energy for conduction and pre-exponential factor of $LiCoO_2$ samples

Precursor mixture	Temperature range/°C	E_a/eV	$\ln\sigma_0 T/(\Omega\text{cm})^{-1}\,\text{K}$
Li_2CO_3–Co_3O_4	600–820	0.370	11.30
	850–900	1.15	20.30
$Li(CH_3COO)\cdot 2H_2O$–Co_3O_4	600–820	0.370	11.60
	850–900	1.15	19.60
Li_2CO_3-basic cobalt carbonate	600–820	0.370	11.40
	850–900	1.15	20.70
$Li(CH_3COO)\cdot 2H_2O$–$Co(CH_3COO)_2\cdot 4H_2O$	600–820	0.369	11.30
	850–900	1.15	20.04

5. Conclusions

Thermoanalytical investigation of the synthesis of $LiCoO_2$ from different precursors provided information on the mechanisms of reaction which can be summarized as follows:

i) the reaction between Li_2CO_3 and Co_3O_4 starts at about $T = 400\,°C$ and slowly proceeds until $T = 700\,°C$, indicating poor reactivity;

ii) in the case of the $Li(CH_3COO)\cdot 2H_2O$–Co_3O_4 mixture the melting of lithium acetate promotes the formation of $LiCoO_2$;

iii) the reaction of Li_2CO_3 with basic cobalt carbonate occurs above $T = 300°C$, after decomposition of cobalt salt to Co_3O_4;

iv) the acetate mixture decomposes into thermal intermediates that readily react at low temperature to give $LiCoO_2$.

The Arrhenius plots for conductivity show semiconducting behaviour for all samples. The activation energies are similar, suggesting that the nature of precursors does not significantly affect the electrical properties of $LiCoO_2$. The temperature-dependence of electrical conductivity shows a jump in the conductivity curve near 850°C, suggesting the existence of a phase transition. The DTA on heating and cooling displays a reversible phase transition with different transition temperatures, indicating a sluggish structural change. The phase transition near 850°C is here assumed to be a spinel–rocksalt type similar to that reported for the system Co_3O_4–CoO and for $Li_{0.35}Co_{2.65}O_4$.

Acknowledgement

We thank Mr. F. Pallini for technical support in the conductivity measurements.

References

[1] T. Ohzuku, A. Ueda, M. Nagayama, Y. Iwakoshi and H. Komori, Electrochim. Acta, 38 (1993) 1159–1167.
[2] L. Plomp, J.B.J. Veldhuis, E.F. Sitters and S.B. van der Molen, J. Power Sources, 39 (1992) 369–373.
[3] J. Molenda, A. Stoklosa and T. Bak, Solid State Ionics, 36 (1989) 53–59.
[4] A. Honders, J.M. der Kinderen, A.H. van Heeren, J.H.W. de Wit and G.H.J. Broers, Solid State Ionics, 14 (1984) 205–216.
[5] K. Mizushima, P.C. Jones, P.J. Wiseman and J.B. Goodenough, Mater. Res. Bull., 15 (1980) 783.
[6] E. Rossen, J.N. Reimers and J.R. Dahn, Solid State Ionics, 62 (1993) 53–60.
[7] P. Barboux, J.M. Tarascon and F.K. Shokooh, J. Solid State Chem., 94 (1991) 185.
[8] M. Yoshio, H. Tanaka, K. Tominaga and H. Noguchi, J. Power Sources, 40 (1992) 347.
[9] C. Delmas, J.J. Braconier and P. Hagenmuller, Mater. Res. Bull., 17 (1982) 117.
[10] ICDD, Powder Diffraction File (inorganic compounds) JCPDS: $LiCoO_2$ [card no 16-427]; Li_2Co_3 [card no 9-359]; Co_3O_4 [card no 9-418]; CoO [card no 9-402].
[11] L.J. van der Pauw, Philips Res. Rep., 13 (1958) 1–9.
[12] W.D. Johnston, R.R. Heikes and D. Sestrich, J. Phys. Chem. Solids, 7 (1958) 1.
[13] R.J. Gummow, M.M. Thackeray, W.I.F. David and S. Hull, Mater Res. Bull., 27 (1992) 327–337.
[14] R.J. Gummow, D.C. Liles and M.M. Thackeray, Mater. Res. Bull., 28 (1993) 235–246.
[15] R.J. Gummow, D.C. Liles and M.M. Thackeray, Mater. Res. Bull., 28 (1993) 1177–1184.
[16] J.T. Richardson and L.W. Vernon, J. Phys. Chem., 62 (1958) 1153–1157.
[17] E. Zhecheva and R. Stoyanova, Mater. Res. Bull., 26 (1991) 1315 1322.